Available online at www.sciencedirect.com

ScienceDirect

journal homepage: www.elsevier.com/locate/he

Assessment of hydrogen fuel for rotorcraft applications

Chana Anna Saias [a,*], *Ioannis Roumeliotis* [a], *Ioannis Goulos* [a], *Vassilios Pachidis* [a], *Marko Bacic* [b]

[a] *Propulsion Engineering Centre, School of Aerospace Transport and Manufacturing, Cranfield University, Bedfordshire, MK43 0AL, UK*

[b] *Rolls-Royce plc, P.O Box 31, Derby, DE24 8BJ, UK*

HIGHLIGHTS

- A civil tilt-rotor is retrofitted for liquid and gaseous hydrogen fuel.
- The hydrogen-fuelled rotorcraft are compared against the kerosene-fuelled counterpart.
- Performance and environmental assessment is conducted at payload-range and mission level.
- Liquid hydrogen offers higher gravimetric densities but its requirement for heating penalizes performance.

GRAPHICAL ABSTRACT

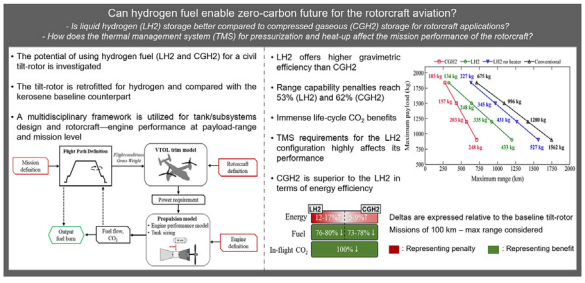

ARTICLE INFO

Article history:
Received 13 May 2022
Received in revised form
26 June 2022
Accepted 30 June 2022
Available online 9 September 2022

Keywords:
Rotorcraft
Tilt-rotor
Hydrogen
Preliminary design
Holistic assessment

ABSTRACT

This paper presents the application of a multidisciplinary approach for the preliminary design and evaluation of the potential improvements in performance and environmental impact through the utilization of compressed (CGH2) and liquefied (LH2) hydrogen fuel for a civil tilt-rotor modelled after the NASA XV-15. The methodology deployed comprises models for rotorcraft flight dynamics, engine performance, flight path analysis, hydrogen tank and thermal management system sizing. Trade-offs between gravimetric efficiency, energy consumption, fuel burn, CO_2 emissions, and cost are quantified and compared to the kerosene-fuelled rotorcraft. The analysis carried out suggests that for these vehicle scales, gravimetric efficiencies of the order of 13% and 30% can be attained for compressed and liquid hydrogen storage, respectively leading to reduced range capability relative to the baseline tilt-rotor by at least 40%. At mission level, it is shown that the hydrogen-fuelled configurations result in increased energy consumption by at least 12% (LH2) and 5% (CGH2) but at the same time, significantly reduced life-cycle carbon emissions compared to the kerosene counterpart. Although LH2 storage at cryogenic conditions has a higher gravimetric efficiency than CGH2 (at 700 bar), it is shown that for this class of rotorcraft, the

* *Corresponding author.*
E-mail address: chana-anna.saias@cranfield.ac.uk (C.A. Saias).

https://doi.org/10.1016/j.ijhydene.2022.06.316

latter is more energy efficient when the thermal management system for fuel pressurization and heating prior to combustion is accounted for.

Nomenclature

Acronyms/Abbreviations

UAM	Urban Air Mobility
VTOL	Vertical Take-Off and Landing
EW	Empty Weight
DP	Design Point
SFC	Specific Fuel Consumption
MTOW	Maximum Take-Off Weight
MLI	Multilayer Insulation
DP	Design Point
RMS	Root-Mean-Square
COPV	Compressed Overwrapped Pressure Vessels
HDPE	High Density Polyethylene
MCR	Maximum Continuous Rating
LH2	Liquefied Hydrogen
CGH2	Compressed Gaseous Hydrogen
FoS	Factor of Safety
TET	Turbine Entry Temperature
PR	Pressure Ratio
LHV	Lower Heating Value

Roman Symbols

AUM_{TO}	All-up-mass at take-off
CO_2	Carbon dioxide
NO_X	Nitrogen-oxides
ETRW	Ratio of energy liberated to revenue work done, $= \frac{W_{fuel} \cdot LHV}{Payload \cdot Range}$
P_{Pump}	Centrifugal pump power (kW)
η_{Pump}	Centrifugal pump efficiency (%)
$P_{Elecheater}$	Electric heater power (kW)
wt	Tank gravimetric density (–)
m_{H2}	Hydrogen fuel mass (kg)
m_{tank}	Hydrogen tank mass (kg)
$\dot{m}_{H2}$	Hydrogen fuel rate (kg/s)
m_{fuel}	Mission fuel burn (kg)
δ_f	Flap angle (deg)
i_N	Nacelle angle (deg)
σ	Material strength (MPa)
P_1	Pump inlet total pressure (bar)
P_2	Pump outlet total pressure (bar)

Introduction

Trends in civil aviation dictate a continuous growth of 4–5% per annum until 2050 [1] based on projections before COVID-19. Passenger transport and air-taxi operations will contribute to this growth, as there is an increasing forecasted demand for passenger transport and Urban Air Mobility (UAM) operations. This new application is envisioned to make use of up to 15-passenger Vertical Take-Off and Landing (VTOL) configurations operating in intra-urban environments for short and frequent flights of 50 nautical miles or less [2].

At the same time, the aviation industry has committed to reducing its carbon emission footprint by half relative to 2005 [1]. The rotorcraft industry contributes to this footprint as currently its operations correspond to 15% of the total commercial airline operations within European airspace [3]. Although the contribution of rotorcraft to the global aviation emissions is currently small, the predicted growth of UAM market could increase it significantly if these vehicles are not carbon neutral. In addition, VTOL serve in densely populated areas and hence, the direct effects of chemical and noise pollutants on humans are aggravated. For this reason, large research and development activities are currently undertaken on novel and sustainable VTOL and propulsion architectures for UAM.

At propulsion level, the research is mainly directed to electrification with fully-electric vehicles more likely to gain wide acceptance for intra-urban operations as they offer zero in-flight carbon emissions [4]. For capacities above four passengers, hybrid-electric solutions are investigated [5,6]. Hybrid-electric propulsion systems offer improved aircraft architectural flexibility, redundancy in case of engine failure, perceived potential for lower maintenance costs and capability to reduce the need for engine oversizing as discussed by Roumeliotis et al. [7]. Additionally, they can potentially contribute to reduced gaseous and noise emissions, factors that are crucial for UAM application. These benefits come at a cost of increased Empty Weight (EW) and complexity of the propulsion and control systems [5]. Current state-of-the-art lithium-ion batteries (250 Wh/kg) severely limit the degree of hybridization if fixed payload-range capacity is to be maintained as demonstrated by Saias et al. [6]. Thus, when retrofitting for practical payloads, fully electric or hybrid-electric VTOL architectures suffer from very low endurance and range [5–8]. To negate this disadvantage, alternative propulsion technologies need to be investigated targeting the reduction of carbon footprint whilst maintaining practical payload-range capability.

The concept of hydrogen fuel for air propulsion has recently gained significant interest as a potential solution to decarbonize aviation. This is due to the fact that when hydrogen is originated by renewable sources, zero carbon and sulfur combustion emissions are produced and only water vapor and small amounts of Nitrogen-oxides [NO_X] are emitted [9,10]. Hydrogen has long been considered due to its

very high specific energy (120 MJ/kg), which is approximately three times greater than that of kerosene [11]. However, conventional aircraft architectures impose weight and volumetric constraints that make hydrogen storage very challenging [12]. This is because the volumetric density of hydrogen in a liquid form is approximately 4 times lower than kerosene, depending on the storage conditions [13]. Thus, retrofitting for hydrogen propulsion may be very limiting and often modifications of the aircraft configuration may become essential [14,15]. Hydrogen tank weight is predominantly affected by hydrogen fuel weight, the storage conditions; pressures and temperatures as well as the geometry and diameter of the tank [16]. According to the literature, these factors have a significant effect on gravimetric efficiency, which can vary from 5% for very low hydrogen masses stored at compressed conditions to approximately 70% for very large hydrogen masses stored at cryogenic conditions [11].

Hydrogen can be stored as compressed gas, liquid or cryo-compressed gas [17]. Liquefied Hydrogen (LH2) storage is the most investigated in the literature for air propulsion due to the high values of gravimetric efficiency ranging from 25% for commuter aircraft [18], 30% for regional [18], 35% for short-range [18] up to 65–70% for long-range applications [11,16,19]. Although LH2 allows for high density and hence high storage efficiency, it comes at a cost of several operational constraints. The design of LH2 storage systems requires a balance between thermal and mechanical requirements as discussed by Verstraete et al. [19]. Hydrogen needs to be liquefied and maintained at cryogenic temperatures (20 K). According to Barthelemy et al. [20], during this process, up to 40% of energy can be consumed. Moreover, a thermal management and control system is essential to minimize boil-off, control pressure inside the tanks, and pressurize and heat hydrogen for combustion [12].

Storing hydrogen in its gaseous state is recognized to be simple and efficient, allowing faster filling compared to liquid hydrogen [12] and hence, has found wider application in the automotive industry [21]. For aircraft applications, the gaseous hydrogen is stored compressed at pressures between 350 and 700 bar [12,21]. The disadvantage of this storage method is the very high volume (due to low density) and high mass of the tank required to withstand the high storage pressures. Specifically, storing at 700 bar results in a 45% increase of the required volume per kg of hydrogen relative to the LH2 storage. Another disadvantage of pressurized tanks is that they involve risks associated with passenger safety [12]. Up to now, gravimetric efficiencies of 13% have been reported based on data on flight-tested vessels in 2009 [22], although the highest commercial tank efficiencies are only of the order of 6% [23]. Recent improvements in materials may be able to contribute to further increasing this value, and potentially make gaseous hydrogen more attractive for short-range aircraft applications.

Safety considerations for both liquid and compressed gaseous hydrogen are primarily directed to the design of the tanks, fuel and thermal management system as well as the supporting infrastructure for safe production and transportation [24]. Hydrogen is associated with a greater likelihood of leaks compared to other fuels due to its high permeability and low viscosity [25]. Moreover, a weaker spark compared to kerosene can cause ignition as hydrogen has a lower minimum ignition energy [26]. Storing hydrogen in cryogenic conditions is associated with increased ignition hazards due to the potential condensation of oxygen in the fuel system components. Thus, the tanks and subsystems must be effectively designed to avoid pressure build-up in the tanks, leaks in the tanks and fuel lines and be mechanically rigid to withstand take-off and landing loads [25]. The positioning of the tanks within the fuselage and their distance from both passengers and other subsystems also play an important role in assuring safe operation [25].

For long-range aircraft applications, liquid hydrogen has been recognized as the only feasible solution due to its higher gravimetric energy efficiency [11,16,19]. Compressed gaseous hydrogen has been identified as impractical for those applications due to the relatively low gravimetric efficiencies [22]. On the other hand, for shorter-range aircraft and rotorcraft applications, compressed tanks have been considered as a potential storage solution [8,27,28]. This is due to the fact that, as hydrogen mass reduces, the gravimetric efficiency reduces, mainly due to the smaller tank diameter making the liquid and gaseous hydrogen gravimetric efficiencies comparable. Verstraete et al. [19] stated that the gravimetric density for a short-range aircraft utilizing liquid hydrogen is expected to reduce by at least 10% compared to long-range applications.

Albeit hydrogen has been identified as a promising fuel and has been covered extensively for fixed-wing aircraft [11,15,16,19], the literature currently available on hydrogen with regards to its application to rotorcraft reveals a knowledge gap. There are no studies in the literature investigating the potential of utilizing hydrogen directly in the gas turbine for rotorcraft and the available studies focus on the utilization of it for hybrid or fully-electric configurations with fuel cells only [8,28]. A holistic assessment of hydrogen technology suitability for VTOL in terms of its implications on overall mission level performance, environmental impact and economy has not been addressed in a multidisciplinary environment. Moreover, a direct comparison of liquid and compressed gaseous hydrogen storage options for rotorcraft with implicit consideration of the tank design and fuel pressurization and heat requirements prior to combustion has not been investigated in the literature.

In light of the research presented in existing literature, hydrogen fuel (compressed and liquid) suitability and feasibility for rotorcraft applications have not yet been evaluated in the literature. This work aims towards closing this gap with the comprehensive exploration and performance assessment of both liquefied and compressed gaseous hydrogen for VTOL configurations. A validated multidisciplinary approach for preliminary design and performance assessment of integrated rotorcraft–powerplant architectures developed by Saias et al. [6,29] is extended to account for hydrogen propulsion. The developed framework comprises models for rotorcraft performance, gas turbine performance as well as models for hydrogen tank and thermal management sizing. It is deployed for the design space exploration and trade-off study of a hydrogen-powered generic tilt-rotor rotorcraft modelled after the NASA XV-15. A comprehensive analysis is presented in terms of the implications of hydrogen-fuelled rotorcraft on payload-range capacity, mission performance, economics, and

environmental impact. This work contributes to the existing literature by providing a deeper insight into the applicability of hydrogen fuel and quantification of its potential performance and environmental benefits relative to a kerosene-fuelled architecture for emerging rotorcraft configurations.

Methodology

An integrated framework for preliminary design and performance assessment of rotorcraft architectures [6,29] is utilized in this paper. The modelling approach comprises a set of comprehensive modules, each applicable to the different aspects of rotorcraft and powerplant performance. Models for rotorcraft performance are coupled with software for engine performance analysis (TURBOMATCH) [30] and a hydrogen tank sizing and weight estimation module. The different simulation models are integrated within a mission analysis module enabling analyses at aircraft and mission levels. Details on the development and validation of the individual methods are presented by Saias et al. [6,29].

Tilt-rotor performance

The integrated modelling approach incorporates the features of the first level of Padfield's hierarchical paradigm, appropriate for performance studies [31]. The rotorcraft module comprises aerodynamic models for the different aircraft components. The rotor model utilizes steady-state non-linear blade element theory [32] coupled with different inflow models for axial propeller flight and flight with an edgewise flow component. The blades are assumed to be rigid bodies, with no flap deflection [32].

In hovering flight, the rotor aerodynamics model is coupled with Bhagwat's inflow model [33]. The method caters to the inclusion of the swirl induced velocity component. In conversion mode, the Mangler and Squire inflow model, a potential flow based analytical model that has found extensive application, is employed [34]. Look-up tables describing the steady-state aerodynamic characteristics for the airfoil sections are deployed.

Experimental look-up tables expressed as functions of incidence and side-slip angles are utilized for the prediction of fuselage and wing-pylon forces and moments [35–37]. The wing is modelled considering the portion of it in the free-stream and slipstream separately as presented in Ref. [38]. The tilt-rotor is a laterally symmetric vehicle that allows to decouple the roll-yaw degrees-of-freedom [39]. A Newton-Raphson approach is applied to obtain the control angles required to achieve an equilibrium trim state for a specified operating condition. The process converges to a set of control inputs to reach equilibrium.

Engine performance (TURBOMATCH)

An in-house engine performance simulation model (TURBOMATCH) [30] has been incorporated into the simulation framework. TURBOMATCH utilizes zero-dimensional aerothermal analysis, employing discrete component maps. It is a well-validated software that has found extensive application and has been deployed in several studies for turboshaft engines for rotorcraft applications [40,41]. It can simulate the engine operation for various fuel types, including hydrogen.

Integrated mission analysis

The mission analysis methodology originally reported by Goulos et al. [40] has been utilized in this work. It is based on the adoption of modular blocks to represent the different mission segments. The rotorcraft and powerplant are assumed to operate at steady-state trim conditions and steady-state off-design conditions for the whole mission, respectively. The flight dynamics code is used to trim the rotorcraft in each segment to calculate the power requirement. The engine fuel flow is calculated, and the weight of the rotorcraft is updated based on the fuel burned at each segment. A fixed-point iteration scheme is employed to solve for mission fuel burn [6,40].

Tilt-rotor and engine model definition

The configuration selected for this study is a civil rotorcraft modelled after the NASA XV-15 [36]. This tilt-rotor configuration combines high-speed cruise and vertical take-off and landing capabilities, which are primary enablers for UAM operations. The XV-15 is equipped with two nacelle-mounted turboshaft engines [36] and has been extensively documented in Refs. [35–37]. Table 1 presents the main design parameters of the rotorcraft. An engine based on General Electric T700-GE-700 suitable for this application is used as the baseline. A detailed description of the T700-GE-700 can be found in Ref. [42]. The maximum power setting is set as the Design Point (DP) as presented in Table 2. The conventional baseline

Table 1 – Tilt-rotor model design parameters [36,37,43].

Design parameter	Value	Units
Empty Weight	4116	kg
MTOW	6803	kg
Disk loading	13.2	lb/ft^2
Number of blades	3	–
Blade radius	3.81	m
Root cut-out	0.0875	%
Blade chord	0.3557	m
Blade twist	41	deg
Rotor solidity	0.089	–
Nominal rotor speed	61.7	rad/s
Turboshaft engine	T700-GE-700	–
Number of engines	2	–

Table 2 – Turboshaft engine model DP at MCR SLS conditions [44].

Design parameter	Value	Units
Design mass flow	4.17	kg/s
Axial compressor PR	5.3	–
Centrifugal compressor PR	2.8	–
TET	1440	K
Fuel flow	0.0807	kg/s
Shaft power	987	kW

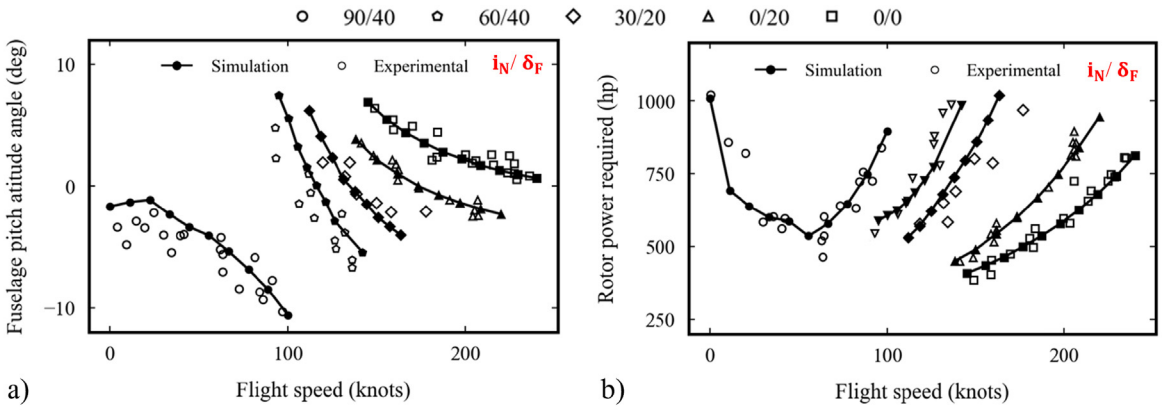

Fig. 1 – Flight dynamics trim results for the XV-15 tilt-rotor – comparison with flight test data [36,45] a) Fuselage pitch angle, b) Single rotor power requirement at different nacelle angles/flap angles at SLS conditions.

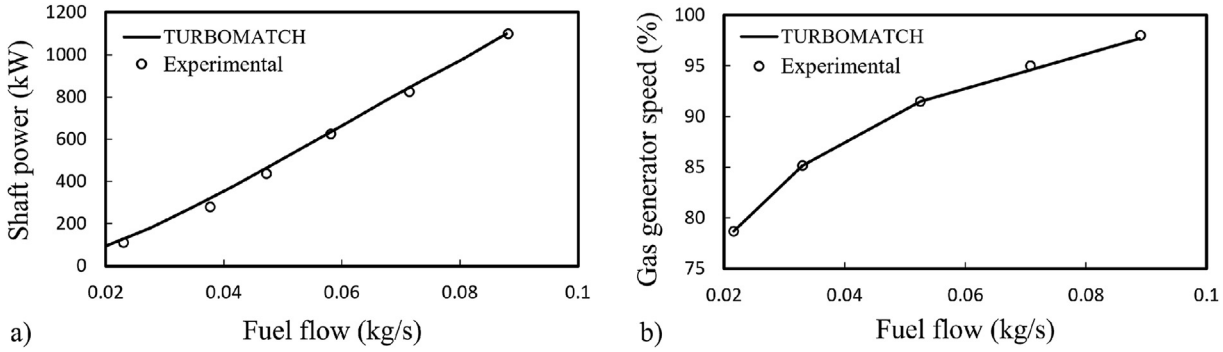

Fig. 2 – TURBOMATCH engine model comparison with measured data [42] for steady-state operation.

tilt-rotor is designed to fly eight sequential short flights of 90 km each.

Tilt-rotor off-design performance

The configuration of interest is validated using experimental and flight test data for the isolated rotors and aircraft trim as presented in Ref. [6]. Predictions for the fuselage pitch angle and rotor power requirement for the XV-15 tilt-rotor operating in straight and level flight are illustrated in Fig. 1 at different nacelle angles (i_N) and flap setting (δ_f). Comparisons with flight test data reported in Ref. [45] are included for validation purposes. Overall, a very good agreement between simulation and flight test data is shown for the prop-rotors at the conditions of interest at near-vertical orientation (90/40) as well as near-horizontal orientation (0/20, 0/0), with a 5.1% and 3.8% Root-Mean-Square (RMS) error relative to the flight test data respectively.

Gas turbine off-design performance

Fig. 2 presents the engine shaft power and gas generator speed with fuel flow rate for the TURBOMATCH T700-GE-700 model developed by Ortiz-Carretero et al. [44] with experimental data extracted from Ref. [42]. The engine model is described and detailed validation is provided in Ref. [44], thus further detail will be omitted.

Hydrogen storage

A methodology based on Colozza [17] and Gangloff [13] was employed to size the hydrogen tanks. Two main constraints can be identified for the storage systems: the tank weight and volume. A parametric analysis is conducted to evaluate the gravimetric efficiency as a function of hydrogen mass to be stored, tank length and diameter targeting to reflect today's technology.

The test-case configuration of this paper imposes several volumetric, weight and engine rating constraints for retrofitting. First, constant power ratings relative to the baseline turboshaft need to be maintained and second, the Maximum Take-Off Weight (MTOW) limits of the rotorcraft need to be satisfied. The wings of the tilt-rotor have restricted space and hence, do not provide sufficient volume to store hydrogen. For this reason, the cylindrical tanks with hemispherical end caps are installed inside the fuselage at the rear side of the rotorcraft.

Fig. 3 illustrates the tilt-rotor configuration and its basic dimensions, where it is highlighted that a feasible tank is limited to a 1.55 m diameter and a 3 m length. The baseline kerosene-fuelled tilt-rotor is designed with a maximum fuel capacity of 675 kg to fly the maximum design mission range. To maintain fixed range capacity, the hydrogen-fuelled tilt-

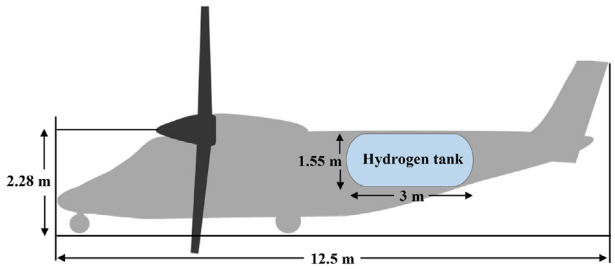

Fig. 3 – Tilt-rotor configuration in longitudinal schematic.

rotor must accommodate integral tanks to carry approximately 242 kg of fuel.

LH2 system sizing

Hydrogen tank. For the case of LH2, the tank design is a trade-off between mechanical and thermal sizing [17,25]. Multilayer insulation (MLI) is selected on account of low boil-off rate [19]. Table 3 demonstrates the main assumptions for the tank design. It is assumed to be stored at 1.45 bar and 21 K. The tank liner is made from Aluminum AL2014 to avoid embrittlement with a minimum thickness of 5 mm due to manufacturing constraints [46] and the outer vessel is assumed to be Stainless Steel 304L [47].

Thermal management. Hydrogen stored in cryogenic conditions requires a thermal management system to pressurize and heat it before combustion. In this work, this system comprises three cryo-pumps per engine for safety as recommended by Brewer [11] for pressurization and an electric heater per engine for heating. Fig. 4 illustrates the T-s diagram for equilibrium hydrogen according to data extracted from Ref. [48], the process 1–2 refers to the pressurization and 2–3 to the heating of the fuel. For the process 1–2, a centrifugal-type pump is selected [11] and sized at take-off that represents the maximum power requirement (Eq. (1)) as seen in Table 4. Hydrogen at the pump inlet is assumed to be a saturated liquid at $P_1 = 1.45$ bar and the outlet is assumed to be $P_2 = 24$ bar (Fig. 4). A variable speed booster pump design in series is selected to achieve higher head. The system weight is calculated to be 40 kg per engine according to Brewer [11].

$$P_{pump} = \dot{m}_{H2}\frac{P_2 - P_1}{\rho_{H2} \cdot \eta_{Pump}} \quad (1)$$

Table 3 – MLI tank design assumptions.

Parameter	Value	Units
Boil-off rate	0.1 [19]	% per hour
Pressure	1.45 [15]	bar
Temperature	21 [15]	K
Ullage	7.2 [15]	%
Factor of safety (FoS)	2.25 [15]	–
$\sigma_{AL_{2014}}$	624 [46]	MPa
$\rho_{AL_{2014}}$	2700 [46]	kg/m^3
$\sigma_{SS_{304L}}$	515 [47]	MPa
$\rho_{SS_{304L}}$	7900 [47]	kg/m^3

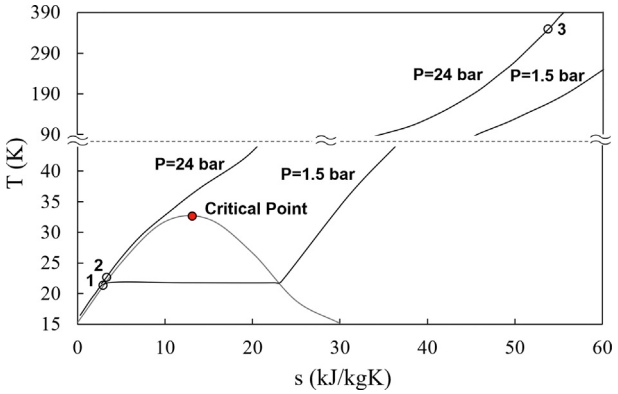

Fig. 4 – T-s diagram for equilibrium hydrogen for temperatures from 15 to 390 K (adapted from Ref. [48]).

Next, the hydrogen heats up prior to combustion through an electric heater. The utilization of an electric heater offers the advantage of a simple design and ensures minimal fluctuations in the injection temperature during operation which is of high importance for efficient combustion [49]. Corchero et al. [50] and Simon et al. [51] reported a low injection temperature limit for hydrogen combustion of 250 K and 150 K, respectively, which is associated with the fuel controller and combustor stability. Although Brewer [11] demonstrated that temperatures around 600 K can be reached with unconventional regenerative cycles, the injection temperature in this study is assumed to be 350 K (point 3 in Fig. 4). This is done in order to have a temperature well above the stability limits [50,51] and at the same time result in a feasible thermal management system design.

The introduction of the electric heater will impose a design constraint on the engine, which must be able to provide sufficient power for the electric heater at every phase of the flight while maintaining constant power ratings relative to the baseline engine. The electric heater is sized at take-off (Eq. (2)) and a power off-take schedule is then generated as a function of power requirement and operating conditions. At take-off, the electric heater requires 115 kW. Thus, to comply with the baseline power ratings (Maximum Continuous Rating (MCR) = 987 kW), the turboshaft engine size increases based on the electric heater power requirements at take-off. Based on this, the gas turbine was scaled up by 11% by scaling the DP inlet mass flow while maintaining the same cycle in terms of specific power. The weight of the electric heater is calculated assuming a 1.15 kW/kg specific power based on a mean value of densities from circulation and immersion heaters [52,53]. The total mass of the thermal management system is 298 kg.

Table 4 – Centrifugal pump sizing conditions.

Parameter	Value	Units
Hydrogen mass flow rate, $\dot{m}_{H2}$	0.0292	kg/s
Pump inlet pressure, P_1	1.45	bar
Pump outlet pressure, P_2	24	bar
Hydrogen density, ρ_{H2}	70.2	kg/m^3
Pump efficiency, η_{Pump}	50 [11]	%

$$P_{Elecheater} = \dot{m}_{H2} \cdot (C_{P_{350}} \cdot T_{350} - C_{P_{21}} \cdot T_{21}) \quad (2)$$

Compressed gaseous hydrogen (CGH2) system sizing

For the compressed hydrogen tanks, Type IV COPV constructed using full composite overwrap were selected on account of high gravimetric efficiency [13]. The compressed vessels are constructed using High Density Polyethylene (HDPE), carbon and glass fiber [13,20]. Based on the hydrogen mass, volume and length-to-diameter ratio, the wall thickness is calculated based on a stress analysis in the circumferential and longitudinal direction of the vessel as presented in Refs. [11,13] and the tank mass is subsequently evaluated. Hydrogen is assumed to be stored at 700 bar and 293 K. At this state, hydrogen density is approximately 40% lower (42.0 kg/m^3) compared to its liquid state considered above. Table 5 presents the main assumptions for the tank design.

Tank design exploration

The tanks are sized based on the hydrogen fuel mass and the length-to-diameter tank ratio, as discussed. Fig. 5 illustrates the design space of the hydrogen tanks that could be integrated into the rotorcraft where the gravimetric efficiency (Equation (3)) of the system is shown as function of tank diameter and hydrogen fuel mass for both LH2 and CGH2. The infeasible designs illustrated in this figure represent tanks that exceed the length or diameter limits imposed by the conventional tilt-rotor (Fig. 3).

$$wt = \frac{m_{H2}}{m_{H2} + m_{tank}} \quad (3)$$

It can be observed that for gaseous hydrogen, the gravimetric efficiency for $m_{H2} = 100–300$ kg varies between 10 and 15%. On the other hand, by storing hydrogen in its liquid state, gravimetric efficiencies of the order of 26–34% can be attained for 100–500 kg of hydrogen fuel. From the same figure, it is observed that the gravimetric efficiency of the LH2 variants is more sensitive to changes in tank diameter and increases for increased diameter. Additionally, it is predominantly affected by the tank diameter rather than the length. These trends represent a broad design space for liquid and compressed hydrogen storage for the investigated architecture, while also including the volumetric constraints of it (Fig. 3).

Table 5 – Compressed overwrapped pressure vessels (COPV) tank design assumptions.

Parameter	Value	Units
Pressure	700 [13]	bar
Temperature	293 [13]	K
Ullage	2.5 [21]	%
Factor of safety (FoS)	2.25 [15]	–
$\sigma_{AL_{T700S}}$	1580 [21]	MPa
$\rho_{AL_{T700S}}$	2300 [21]	kg/m^3

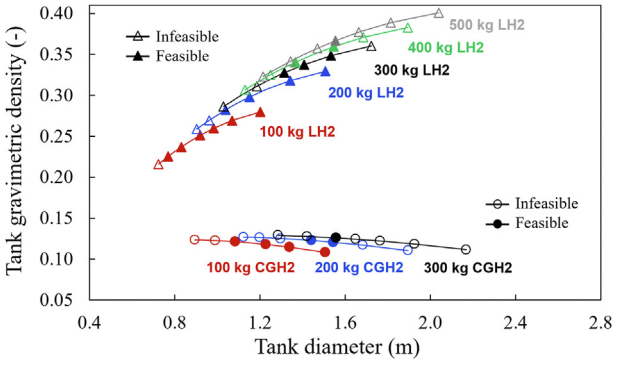

Fig. 5 – Hydrogen tank design space utilizing compressed gas and liquid hydrogen for the civil tilt-rotor.

Results & discussion

An assessment at payload-range and mission level was carried out to comprehend the impact of hydrogen fuel on performance, life-cycle CO_2 and economics for a civil tilt-rotor configuration. The hydrogen-fuelled architectures designed with LH2 and CGH2 are first evaluated and compared with the kerosene-fuelled rotorcraft at payload-range level. Next, the hydrogen storage system is re-designed at different payload levels, highlighting trade-offs between weight, endurance, economy, energy efficiency and carbon footprint. Finally, the overall performance of the hydrogen-fuelled rotorcraft are assessed and compared within a holistic environment for off-design mission scenarios.

Payload-range comparison

Fig. 6 illustrates the payload-range diagram for the conventional baseline and hydrogen-fuelled tilt-rotors. The maximum fuel capacity is annotated for each configuration in this figure. The tanks are sized with respect to the volumetric constraints of the rotorcraft as well as its weight constraint to never exceed the baseline MTOW. The payload-range diagram is constructed based on the sizing mission of the baseline rotorcraft illustrated in Fig. 7. It consists of a 5-min idle period, a take-off and climb segment up to 1000 m altitude and a subsequent descent and land segment. The mission time depends on the configuration and range that the rotorcraft can fly and hence, varies between 38 and 112 min (Fig. 7).

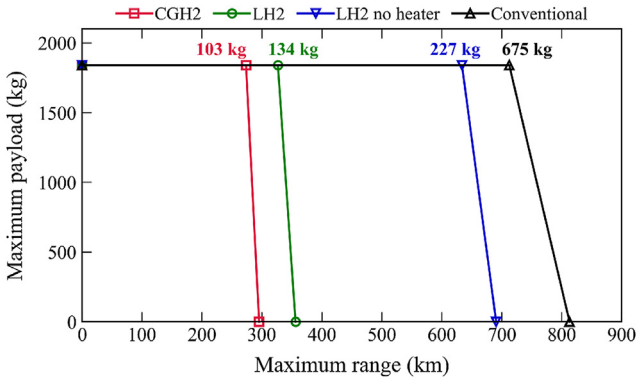

Fig. 6 – Payload-range diagram of hydrogen-fuelled and kerosene-fuelled tilt-rotor rotorcraft.

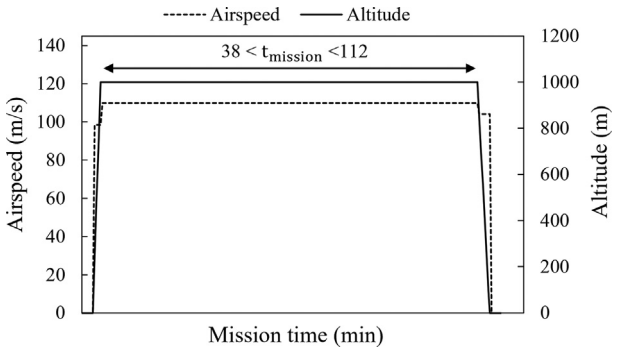

Fig. 7 – Mission altitude and flight speed profile for the sizing mission.

The kerosene-fuelled tilt-rotor carries 675 kg of fuel to complete the design mission. To maintain the same on-board energy, approximately 242 kg of hydrogen need to be integrated within the retrofitted tilt-rotor. From Fig. 6 it is observed that the maximum fuel that can be stored in the CGH2 configuration is 103 kg, resulting in a reduced range by 62% relative to the kerosene-fuelled counterpart. This penalty in range is attributed to the low gravimetric efficiency of the CGH2 storage system (12.6%) that leads to reduced on-board energy relative to the kerosene counterpart. For the LH2 configuration, two variants are designed in an effort to effectively decouple the thermal management effects on the overall performance of the system. Thus, first, a liquid hydrogen-fuelled variant without accounting for the thermal management requirements is designed (LH2 no heater). Second, a variant comprising a pressurization system and an electric heater to compress and preheat hydrogen is designed (LH2). It is highlighted that in order to isolate the thermal management system effects, both LH2 variants are assumed to have a fixed fuel inlet temperature of 350 K as discussed in Section LH2 system sizing. It is observed that the LH2 no heater rotorcraft can carry 227 kg at maximum payload capacity resulting in an 11% reduced range relative to the baseline tilt-rotor. For the LH2 configuration on the other hand, the maximum fuel capacity reduces to 134 kg. At this point, the maximum range is penalized by 53% relative to the baseline. It is therefore realized that although the gravimetric efficiency of the LH2 configuration is approximately two times higher than the CGH2, the added weight of the thermal management system, as well as the need to increase the engine size to maintain the same power ratings, affect the performance significantly and hence, should not be neglected. The thermal management system could be improved by introducing a regenerative cycle to take advantage of the high-temperature exhaust gases to preheat fuel. Thus, a more efficiently designed system will be situated in between the two liquid hydrogen variants considered in this study.

It was demonstrated that the integration of hydrogen tanks comes at a cost of reduced range capability. On the other hand, hydrogen offers the potential to improve fuel economy and eliminate carbon emissions. To directly compare the configurations of interest, holistic metrics accounting for payload and range capability as well as fuel economy and environmental impact must be used. Thus, the ratio of energy liberated to revenue work done (ETRW), a metric introduced by Poll [54] (Equation (4)) is used for comparison at energy level. Similarly, the fuel, cost and life-cycle CO_2 are expressed as ratios per range flown per passenger capacity for comparison purposes as presented in Table 6.

$$ETRW = \frac{m_{fuel} \cdot \mathrm{LHV}}{Payload \cdot Range} \tag{4}$$

A first observation is that the kerosene-fuelled configuration results in the lowest energy consumption per range flown compared to all hydrogen variants. This is attributed first to the increased empty weight of the hydrogen configurations due to the storage system and second, to the lower weight reduction rate of the hydrogen configuration during the mission due to the lighter fuel burned. Consequently, the take-off weight is fixed for all the configurations but, all hydrogen variants are heavier compared to the kerosene-fuelled tilt-rotor throughout the mission resulting in higher thrust requirements and hence, fuel consumption. It is also observed that the LH2 configuration without the thermal management system results in a 5.3% penalty in ETRW relative to the baseline tilt-rotor. This increases to 20.6% when the electric heater is integrated into the system highlighting the significant effect of the pressurization and heating system on energy efficiency. This is attributed first to the increase in EW due to the added system (pumps and electric heater) that results in less available space and weight margin for hydrogen fuel storage. Second, the thermal management requirements for fuel pumping and preheating before combustion require the installation of a larger engine to comply with the baseline power ratings and the off-take electric heater requirement resulting in the engine working at less favorable operating points throughout the mission. Finally, the power off-take requirement for the electric heater also increases fuel consumption during the whole mission.

The CGH2 variant results in a 10.7% increase in ETRW relative to the kerosene-fuelled tilt-rotor. Therefore, when ignoring the thermal management system and its weight and

Table 6 – Comparison of configurations of interest at the payload-range mission at maximum payload level. Life-cycle CO_2 emissions calculated based on estimates reported in Refs. [55,56].

Configuration	ETRW $(\frac{MJ}{kg \cdot km})$	$\frac{m_{fuel}}{P \cdot R}$ $(\frac{g}{kg \cdot km})$	$\frac{CO_2}{P \cdot R}$ $(\frac{g}{kg \cdot km})$	$\frac{Cost}{P \cdot R}$ $(\frac{USD}{kg \cdot km})$
			Life-cycle **(In-flight)**	
Conventional	0.022	0.515	2.346 **(1.617)**	0.026
LH2 no heater	0.023	0.195	0.467 **(0)**	0.031
LH2	0.027	0.223	0.535 **(0)**	0.036
CGH2	0.025	0.205	0.491 **(0)**	0.033

power implications, the hydrogen variant (LH2 no heater) is superior compared to the CGH2 and LH2 variants in terms of ETRW. However, when the thermal management system is included, an opposite trend is observed with the CGH2 being more energy-efficient compared to the LH2 tilt-rotor. This highlights the importance of the inclusion of the thermal management requirements for short-range applications as it may have an important impact on the potential selection of storage system.

Next, the designed configurations are compared at CO_2 level. Albeit hydrogen combustion eliminates in-flight CO_2 emissions, life-cycle CO_2 emissions associated with hydrogen production, transfer and equipment maintenance need to be accounted for. Thus, the CO_2 considered for this comparison includes CO_2 emitted during flight for the kerosene-fuelled tilt-rotor as well as CO_2 resulting from production and transportation for both the hydrogen and conventional tilt-rotor (Table 6). According to Cetinkaya, hydrogen produced by water electrolysis via photovoltaic energy results in 2.4 kg of CO_2/kg of hydrogen fuel [55]. At the same time, the production of kerosene via conventional crude oil results in 1.4 kg of CO_2/kg of jet A [56]. Thus, the calculation of the life-cycle carbon emissions is based on the above estimates.

It is observed that the hydrogen-fuelled architectures lead to significant reductions in CO_2 relative to the kerosene counterpart with benefits varying from 77% to 79% for the LH2 and CGH2, respectively. Similarly, reductions in fuel burn per passenger and range flown are observed of the order of 60% for the CGH2, and 57% and 62% for the liquid variant with and without the electric heater, respectively.

To conclude, the liquid hydrogen configuration without a thermal management system (LH2 no heater) results in greater range capability, fuel economy and environmental impact compared to the CGH2. However, when the thermal management system is considered, the LH2 allows for higher range capability at maximum payload at a penalty of 9% increase in fuel and CO_2 per payload-range relative to the CGH2 variant. The dominant factor for this increase is the larger engine operating at a less efficient average point during the mission and hence, higher Specific Fuel Consumption (SFC).

In the present comparison, the cost of the mission is considered by accounting for the fuel supply chain, infrastructure for fuel production, transportation and refueling in Europe as predicted in Ref. [18]. Based on estimates for 2025, the cost of kerosene and hydrogen will be 50 USD/kg and 160 USD/kg, respectively [18]. From Table 6, it is observed that despite the significant reduction that the hydrogen configurations offer in block fuel, the kerosene-fuelled tilt-rotor results in the lowest cost. The highest penalty observed is a 36% increase for LH2 tilt-rotor relative to the baseline. The CGH2 tilt-rotor on the other hand results in 27% higher overall cost compared to the kerosene counterpart. It is noted however that, due to the existence of various production sources for hydrogen, it is expected that the fuel price will gradually decrease after 2025 and will be stabilized in the next ten years [18]. Based on this assessment, the break-even point towards cost parity with the kerosene tilt-rotor is 115 USD/kg and 125 USD/kg for the LH2 and the CGH2 tilt-rotor, respectively.

Trade-off analysis at payload-range level

As presented in Section Payload-range comparison, maintaining a fixed payload relative to the baseline architecture severely limits the maximum hydrogen capacity for a retrofit scenario on the existing platform leading to impractical range capabilities. For this reason, the impact of reducing payload to integrate larger tanks and hence, increase range capability in the system is investigated. Fig. 8 a) illustrates the payload-range trade-off of the CGH2 tilt-rotor with the hydrogen tanks re-designed at each payload level starting from the maximum (1840 kg) to the minimum (900 kg). Each point on this plot represents a unique tilt-rotor configuration that has been sized to carry the maximum hydrogen fuel on board and next, a payload-range diagram is constructed at each payload level. It is highlighted that the configurations are designed to comply with the baseline power ratings and the volumetric and weight constraints of the baseline rotorcraft.

From Fig. 8 a), it is observed that as the maximum payload reduces, the hydrogen capacity increases allowing for higher range capability. The red dashed line represents the maximum fuel storage level that the rotorcraft can carry at each payload level. The maximum fuel capacity is annotated in the plot for the kerosene and hydrogen aircraft. It is observed that carrying 65% of the original payload allows for the CGH2 configuration to fly 80% of the original design range. For even lower payload capacities close to 50% relative to the baseline, the CGH2 tilt-rotor can fly the original range. Hydrogen masses above 300 kg cannot be stored in the tilt-

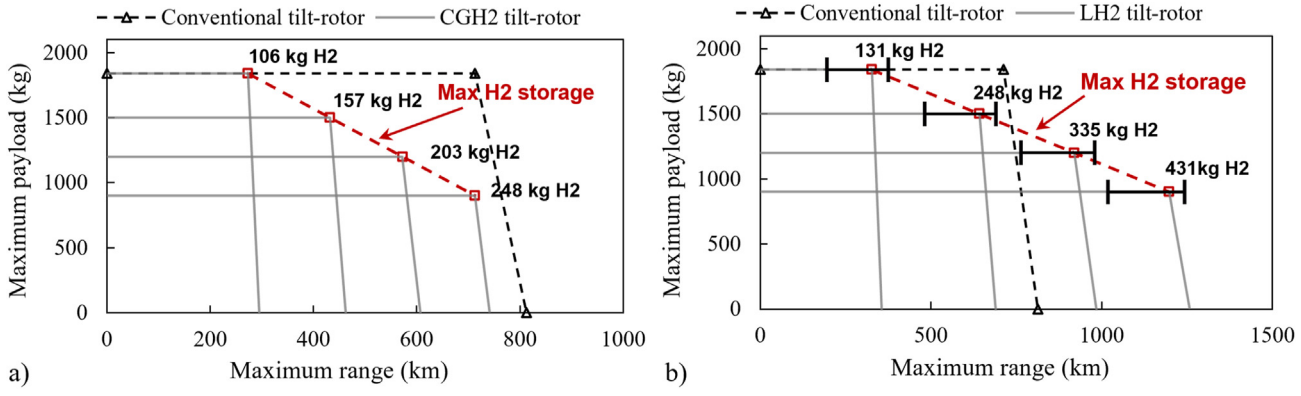

Fig. 8 – Payload-range trade-off of the a) CGH2 and b) LH2 tilt-rotor for various fuel storage levels.

rotor as the tank volume exceeds the limits of the architecture (Fig. 3).

Fig. 8 b) illustrates the payload-range trade-off for the LH2 tilt-rotor. Similarly to Fig. 8 a), at each level of payload, the rotorcraft is sized with respect to the maximum fuel that can be stored and the red dashed line represents the maximum liquid hydrogen capacity. An error band is displayed in black to account for potential variation in the power density of the electric heater. A mean value of 1.15 kW/kg power density is used with limits of varying from 0.5 kW/kg [52] to 1.8 kW/kg [53]. The effect of power density for the lower limit (0.5 kW/kg) is significant as the increased weight heavily penalizes the hydrogen fuel capacity and hence, the range capability of the rotorcraft. This effect is more pronounced at high payload levels. As discussed, liquid hydrogen storage has a much higher gravimetric efficiency and a density of approximately 40% higher compared to the gaseous state. This results in higher ranges at each level of payload. Moreover, the maximum hydrogen fuel that can be stored (431 kg) in the LH2 tilt-rotor is greater compared to the CGH2 variants. Carrying 1500 kg of payload allows flying 90% of the original range with 248 kg of hydrogen. For lower payload capacities, the maximum range that the rotorcraft can fly can exceed the original range.

A comparison of the maximum fuel capacity line seen in Fig. 8 a)-8 b) for the baseline kerosene-fuelled and hydrogen-fuelled variants is illustrated in Fig. 9. At each payload level, the tanks are uniquely designed to carry the maximum fuel possible and integrated into the system without violating any weight or volumetric constraints and maintaining AUM_{TO} = MTOW.

For the hydrogen variants, as payload reduces, greater masses of hydrogen can be stored and hence, the total installed energy of the system increases. Similarly, for the baseline tilt-rotor, as maximum payload reduces, the available fuel that the tilt-rotor can carry increases. The fuel stored at the beginning of the mission is annotated for all the configurations at 1840 kg, 1500 kg, 1200 kg and 900 kg of payload. From this figure, it is observed that the rate of increase in range of the two LH2 variants is higher compared to the CGH2 variant. This is due to the fact that as the mass of fuel increases, the gravimetric efficiency increases and hence, the storage system weight penalty becomes smaller allowing more fuel on board for the LH2 configurations (Fig. 5). On the other hand, the gravimetric efficiency for the CGH2 tanks is less sensitive to fuel mass and therefore, there is a marginal benefit at reduced payload capacity.

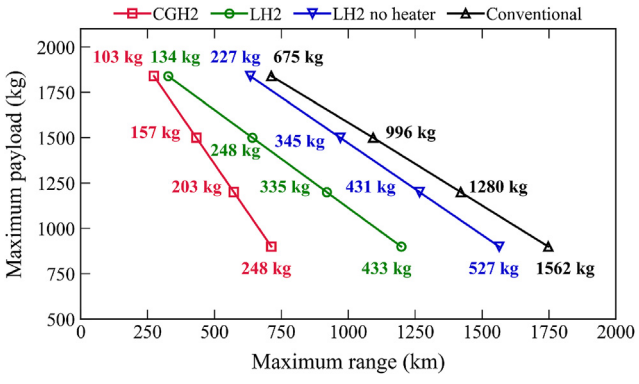

Fig. 9 – Comparison of payload-range capacity for conventional and hydrogen-fuelled tilt-rotor configurations (AUM_{TO} = const).

Two payload levels are considered for comparison against the baseline, them being the maximum payload (1840 kg) and a 20% reduced payload (1500 kg) targeting to maintain a range close to the design range of the conventional tilt-rotor (Table 7). It is observed that at both payload levels, the kerosene-fuelled tilt-rotor is the most energy-efficient. Penalties in the energy of the order of 5% and 10% are observed for the LH2 without the electric heater configuration and the CGH2 configuration, respectively. The highest energy penalty relative to the baseline tilt-rotor (18–20%) is observed for the LH2 configuration which is attributed to the increase in EW and operation at a higher SFC throughout the mission due to the thermal management system integration.

The thermal management penalty also affects life-cycle CO_2 emissions of the LH2 tilt-rotor. Although hydrogen-fuelled configurations can eliminate carbon emissions during flight, the production and transportation of fuel will have an impact on carbon emissions and hence, it is also accounted for in the analysis. From Table 8, it is observed that the LH2 tilt-rotor without the electric heater results in the lowest carbon footprint compared to the rest of the configurations for both payload levels. For the LH2 and CGH2 configurations the CO_2 benefits reach 77% and 79%, respectively.

Mission level assessment

As the tilt-rotor is expected to fly for shorter mission ranges than the design range, an analysis is carried out for off-design missions to evaluate the impact of range on energy, fuel economy, cost and carbon emissions. It was demonstrated in Section Payload-range comparison that maintaining maximum payload results in reduced range capability by at least 60%. For this reason, for the present analysis, a reduced

Table 7 – Percentage delta variation of the ETRW relative to the conventional tilt-rotor.

Configuration	Percentage delta ETRW relative to the conventional (%)	
	PAX = 1840 kg	PAX = 1500 kg
LH2 no heater	5.3	5.5
LH2	20.6	18.1
CGH2	10.7	10.9

Table 8 – Percentage delta variation of CO_2 gaseous emissions relative to the conventional tilt-rotor.

Configuration	Percentage delta CO_2 relative to the conventional (%)	
	PAX = 1840 kg	PAX = 1500 kg
LH2 no heater	−80.1	−80.0
LH2	−77.2	−77.7
CGH2	−79.1	−79.0

payload capacity of 1500 kg is selected targeting the investigation of a broader range of missions. As discussed, the gas turbine remains the same for the CGH2 and LH2 no heater variants and is scaled up for the LH2 variant.

Fig. 10 illustrates the block fuel of the baseline and hydrogen-fuelled tilt-rotor for various mission ranges. It can be observed that the LH2 configuration without any thermal management penalties can fly two times longer than the CGH2 variant due to its higher gravimetric efficiency. On the other hand, when the electric heater is included, the difference in the range becomes 50% relative to the CGH2 configuration. Additionally, it is observed that the CGH2 configuration results in better fuel economy compared to the LH2 configuration. Specifically, the CGH2 variant consumes 5–7% less fuel compared to the LH2 tilt-rotor depending on the mission range. This is attributed to two main factors. First, the CGH2 variant operates at an average mission thermal efficiency of 24% compared to 21.3% for the LH2 tilt-rotor due to the integration of a bigger engine and the off-take to power the electric heater. Second, the LH2 tilt-rotor has a fuel useable fraction of 93% compared to the 97% of the CGH2. As expected, all the hydrogen variants result in lower block fuel and hence, CO_2 emissions relative to the baseline tilt-rotor.

Since the two fuels have different calorific values, the configurations of interest are compared at an energy level per payload and range as depicted in Fig. 11. It is observed that the baseline configuration results in the lowest block energy compared to all the hydrogen-fuelled variants. It is highlighted that at this payload capacity, the kerosene-fuelled architecture operates with a lower take-off weight especially at shorter ranges. For this reason, the penalties of the hydrogen variants are greater at low mission ranges.

It is observed that the CGH2 configuration results in penalties that vary between 8.9% and 5.2% for mission ranges starting from 100 to 432 km. The hydrogen-fuelled tilt-rotor without the electric heater (LH2 no heater) on the other hand leads to increased energy consumption that varies from 5.8% to a minimum of 2.6% for missions of 100–970 km respectively. The introduction of the thermal management system further increases the penalty to 17% at 100 km and 12.1% at 645 km. It is realized that for lower ranges, the difference between the hydrogen and kerosene variants becomes more obvious, as the baseline rotorcraft operates at lower take-off

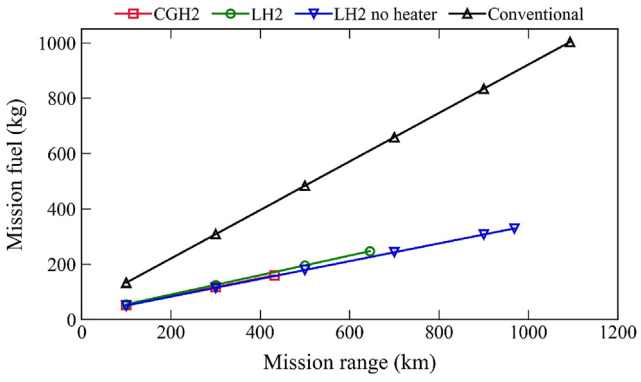

Fig. 10 – Comparison of mission fuel for the conventional and hydrogen-fuelled tilt-rotor architectures at various mission ranges for 1500 kg of payload.

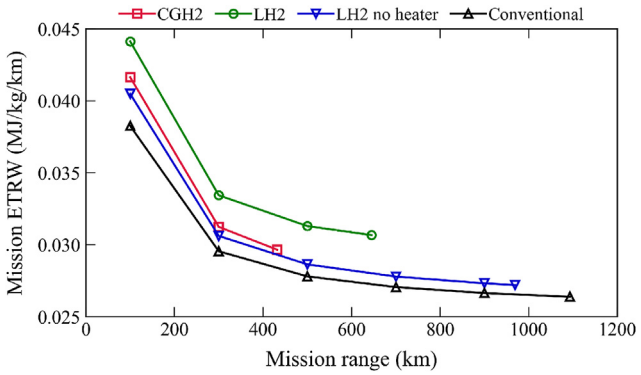

Fig. 11 – Comparison of mission energy per payload and range for the conventional and hydrogen-fuelled tilt-rotor architectures at various mission ranges for 1500 kg of payload.

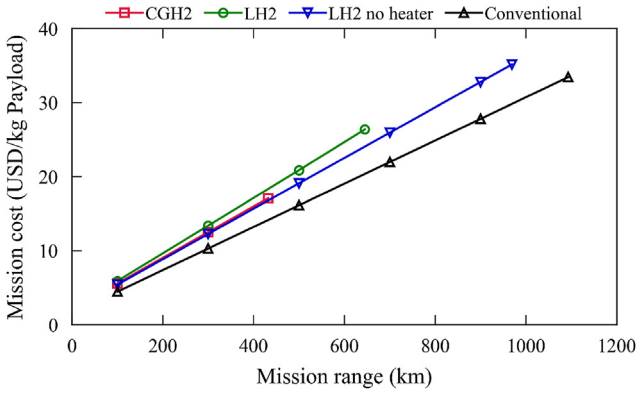

Fig. 12 – Comparison of mission fuel cost per passenger for the conventional and hydrogen-fuelled tilt-rotor architectures at various mission ranges for 1500 kg of payload.

weights for all the missions considered. As the mission range increases, the energy penalties of the hydrogen configurations relative to the baseline tend to reduce due to the variation of gross weight throughout the mission. From Fig. 12, it is concluded that the kerosene-fuelled configuration is the most economical solution for all mission ranges considered based on cost projections for 2025 [18] followed by the LH2 no heater, CGH2 and LH2.

Conclusions

This work presented a comprehensive investigation of the suitability of hydrogen fuel for VTOL air-taxi configurations. A multidisciplinary approach for preliminary design and performance analysis of integrated rotorcraft–hydrogen powerplant architectures was deployed. The framework is used for performance analysis at mission level to quantify corresponding trade-offs between fuel economy, energy efficiency, carbon emissions and thermal management, hydrogen tank, and rotorcraft weight. The overall methodology was applied to a generic civil tilt-rotor modelled after the NASA XV-15.

A validated kerosene-fuelled tilt-rotor model is used for retrofitting with hydrogen propulsion. Both liquid and gaseous hydrogen storage options are explored. Simplified models are used for the design and weight estimation of the hydrogen tank and thermal management systems. The performance benefits and associated penalties of hydrogen compared to the kerosene counterpart were investigated and quantified at aircraft, payload-range and mission level. For this application, gravimetric efficiencies of the order of 27–36% for LH2 and 12–13% for CGH2 depending on the fuel capacity. At payload-range level, it was demonstrated that to maintain the maximum payload (1500 kg) of the baseline kerosene-fuelled architecture, the range capability of the hydrogen rotorcraft must decrease by 62% (CGH2) and 53% (LH2) of the original range depending on the storage type. As payload progressively reduces, larger masses of hydrogen can be stored and hence, the range that the rotorcraft can fly increases.

At mission level, it was demonstrated that all hydrogen variants result in increased block energy relative to the kerosene-fuelled tilt-rotor due to the increased EW and lower weight reduction rate due to the lower fuel masses during flight. The penalties are more pronounced for low mission ranges. Specifically, when designed for 1500 kg payload, the LH2 variant results in increased ETRW relative to the baseline by 12% at maximum range (645 km) and 17% at 100 km. The CGH2 architecture results in higher ETRW by 5% at maximum range (432 km) and 9% at 100 km. Both hydrogen configurations lead to immense benefits in life-cycle CO_2 emissions accounting for in-flight and production, storage, and transportation CO_2 despite the increase in rotorcraft EW. Based on cost projections for 2025, kerosene fuel is the most economical solution offering at least a 20% lower overall mission cost relative to the hydrogen variants.

It has been demonstrated that although the LH2 configuration results in higher range capability due to higher gravimetric efficiency, the CGH2 comes with a better energy efficiency when the LH2 thermal management system is accounted for. This is because the LH2 configuration requirements for pressurization and heating result in increased EW and necessitates the integration of a larger engine which heavily penalizes thermal efficiency. It was highlighted that including the thermal management penalties at preliminary design level allows understanding the feasible boundaries as well as the realistic benefits and penalties of such systems. Additionally, for short-range applications, the inclusion of those requirements plays a critical role in the selection of the storage type (liquid or compressed). Consequently, further investigations covering thermal management aspects are highly recommended for preliminary and detailed design phases for these applications.

This work has provided new insight into the suitability of hydrogen fuel directly injected in the gas turbine for rotorcraft architectures and its associated trade-offs in overall performance and environmental impact. The trends provided present a valuable design space for integrated rotorcraft–hydrogen powerplant and storage system with implicit consideration of weight, volume constraints, and thermal management requirements. The present analysis can be adapted in the future to account for technological advancements that will allow attaining higher gravimetric efficiencies and more effective thermal management approaches.

Credit author statement

Saias Chana Anna: Conceptualization, Methodology, Software, Validation, Visualization, Writing - Original Draft. **Ioannis Roumeliotis:** Conceptualization, Supervision, Writing - Review & Editing. **Ioannis Goulos:** Supervision, Writing - Review & Editing. **Vassilios Pachidis:** Supervision, Writing - Review & Editing. **Marko Bacic:** Supervision, Writing - Review & Editing.

Declaration of competing interest

The authors declare that they have no known competing financial interests or personal relationships that could have appeared to influence the work reported in this paper.

Acknowledgements

The authors would like to express their gratitude to Rolls-Royce plc. for funding this research and for permission to publish the paper.

REFERENCES

[1] International Air Transport Association (IATA). Aircraft technology roadmap to 2050, Technical Report ARC R & M 2642. URL, https://www.iata.org/contentassets/8d19e716636a47c184e7221c77563c93/Technology-roadmap-2050.pdf.

[2] Holden J, Goel N. Fast-forwarding to a future of on-demand urban air transportation, White Paper, Uber.

[3] D'Ippolito R, Stevens J, Pachidis V, Berta A, Goulos I, Rizzi C. A multidisciplinary simulation framework for optimization of rotorcraft operations and environmental impact. In: 2nd International conference on engineering optimization. Lisbon: Portugal; 2012. p. 1–11.

[4] Edwards T, Price G. "eVTOL Passenger Acceptance," Technical Report NASA/CR—2020–220460. Jan 2020 [Online]. Available: https: //ntrs.nasa.gov/citations/20200000532.

[5] Danis RA, Green MW, Freeman JL, Hall DW. Examining the conceptual design process for future hybrid-electric rotorcraft, Technical Report, NASA/CR-2018-219897. p. 1–81.

[6] Saias CA, Goulos I, Roumeliotis I, Pachidis V, Bacic M. Preliminary design of hybrid-electric propulsion systems for emerging urban air mobility rotorcraft architectures. J Eng Gas Turbines Power 2021;143(11):111015. https://doi.org/10.1115/1.4052057. https://asmedigitalcollection.asme.org/gasturbinespower/article-pdf/143/11/111015/6765892/gtp_143_11_111015.pdf.

[7] Roumeliotis I, Mourouzidis C, Zafferetti M, Unlu D, Broca O, Pachidis V. Assessment of thermo-electric power plants for rotorcraft application. J Eng Gas Turbines Power 2020;142(5):051003. https://doi.org/10.1115/1.4045103.

[8] Ng W, Datta A. Hydrogen fuel cells and batteries for electric-vertical takeoff and landing aircraft. J Aircraft 2019;56(5):1765–82. https://doi.org/10.2514/1.C035218.

[9] Akçay I, Gürbüz H, Akçay H, Aldemir M. An investigation of euro diesel-hydrogen dual-fuel combustion at different speeds in a small turbojet engine. Aircraft Eng Aero Technol 2021;93:701–10. https://doi.org/10.1108/AEAT-10-2020-0235.

[10] Gürbüz H, Akçay H, Aldemir M, Akçay İH, Topalcı Ü. The effect of euro diesel-hydrogen dual fuel combustion on performance and environmental-economic indicators in a small uav turbojet engine. Fuel 2021;306:121735. https://doi.org/10.1016/j.fuel.2021.121735. URL, https://www.sciencedirect.com/science/article/pii/S0016236121016161.

[11] Brewer GD. Hydrogen aircraft technology. Boca Raton: CRC Press; 1991.

[12] Baroutaji A, Wilberforce T, Ramadan M, Olabi AG. Comprehensive investigation on hydrogen and fuel cell technology in the aviation and aerospace sectors. Renew Sustain Energy Rev 2019;106:31–40. https://doi.org/10.1016/j.rser.2019.02.022. URL, https://www.sciencedirect.com/science/article/pii/S1364032119301157.

[13] Gangloff J, John J, Kast J, Morrison G, Marcinkoski J. Design space assessment of hydrogen storage onboard medium and heavy duty fuel cell electric trucks. J Electrochem En Conv Stor 2017;14(2):021001. https://doi.org/10.1115/1.4036508.

[14] Nicolay S, Karpuk S, Liu Y, Elham A. Conceptual design and optimization of a general aviation aircraft with fuel cells and hydrogen. Int J Hydrogen Energy 2021;46(64):32676–94. https://doi.org/10.1016/j.ijhydene.2021.07.127. URL, https://www.sciencedirect.com/science/article/pii/S0360319921027920.

[15] Winnefeld C, Kadyk T, Bensmann B, Krewer U, Hanke-Rauschenbach R. Modelling and designing cryogenic hydrogen tanks for future aircraft applications. Energies 2021;11(1). https://doi.org/10.3390/en11010105.

[16] Huete J, Pilidis P. Parametric study on tank integration for hydrogen civil aviation propulsion. Int J Hydrogen Energy 2021;46(74):37049–62. https://doi.org/10.1016/j.ijhydene.2021.08.194. URL, https://www.sciencedirect.com/science/article/pii/S0360319921034418.

[17] Colozza AJ, Kohout LL. Hydrogen storage for aircraft applications overview. Tech. Rep. NASA/CR-2002-211867 September 2002.

[18] CleanSky2. Hydrogen-powered aviation. A fact-based study of hydrogen technology, economics, and climate impact by 2050. Tech. rep May 2020 [96 pages]. URL, https://www.fch.europa.eu/sites/default/files/FCH%20Docs/20200507_Hydrogen%20Powered%20Aviation%20report_FINAL%20web%20%28ID%208706035%29.pdf. In preparation.

[19] Verstraete D, Hendrick P, Pilidis P, Ramsden K. Hydrogen fuel tanks for subsonic transport aircraft. Int J Hydrogen Energy 2010;35(20):11085–98. https://doi.org/10.1016/j.ijhydene.2010.06.060. hyceltec 2009 Conference, https://www.sciencedirect.com/science/article/pii/S036031991001236X.

[20] Barthelemy H, Weber M, Barbier F. Hydrogen storage: recent improvements and industrial perspectives. Int J Hydrogen Energy 2017;42(11):7254–62. https://doi.org/10.1016/j.ijhydene.2016.03.178. special issue on The 6th International Conference on Hydrogen Safety (ICHS 2015), 19-21 October 2015, Yokohama, Japan, https://www.sciencedirect.com/science/article/pii/S0360319916305559.

[21] Hua T, Ahluwalia R, Peng J-K, Kromer M, Lasher S, McKenney K, Law K, Sinha J. Technical assessment of compressed hydrogen storage tank systems for automotive applications. Int J Hydrogen Energy 2011;36(4):3037–49. https://doi.org/10.1016/j.ijhydene.2010.11.090. URL, https://www.sciencedirect.com/science/article/pii/S0360319910023050.

[22] Gong A, Verstraete D. Fuel cell propulsion in small fixed-wing unmanned aerial vehicles: current status and research needs. Int J Hydrogen Energy 2017;42(33):21311–33. https://doi.org/10.1016/j.ijhydene.2017.06.148. URL, https://www.sciencedirect.com/science/article/pii/S036031991732503X.

[23] Yoshida T, Kojima K. Toyota MIRAI fuel cell vehicle and progress toward a future hydrogen society. Interface magazine 2015;24(2):45–9. https://doi.org/10.1149/2.f03152if.

[24] Hoelzen J, Silberhorn D, Zill T, Bensmann B, Hanke-Rauschenbach R. Hydrogen-powered aviation and its reliance on green hydrogen infrastructure – review and research gaps. Int J Hydrogen Energy 2022;47(5):3108–30. https://doi.org/10.1016/j.ijhydene.2021.10.239. hydrogen Energy and Fuel Cells, https://www.sciencedirect.com/science/article/pii/S0360319921043184.

[25] Rompokos P, Rolt A, Nalianda D, Sibilli T, Benson C. Cryogenic fuel storage modelling and optimisation for aircraft applications, vol. Volume 6: ceramics and ceramic composites; Coal, Biomass, Hydrogen, and Alternative Fuels; Microturbines, Turbochargers, and Small Turbomachines of Turbo Expo: Power for Land, Sea, and Air. 2021. v006T03A001. arXiv:https://asmedigitalcollection.asme.org/GT/proceedings-pdf/GT2021/84997/V006T03A001/6758309/v006t03a001-gt2021-58595.pdf.

[26] Khandelwal B, Karakurt A, Sekaran PR, Sethi V, Singh R. Hydrogen powered aircraft : the future of air transport. Prog Aero Sci 2013;60:45–59. https://doi.org/10.1016/j.paerosci.2012.12.002. URL, https://www.sciencedirect.com/science/article/pii/S0376042112000887.

[27] Husemann M, Glaser CK, Stumpf E. Assessment of a fuel cell powered air taxi in urban flight conditions. 2019, AIAA 2019-0812, Electric Aircraft Design Concepts I. arXiv: https://arc.aiaa.org/doi/pdf/10.2514/6.2019-0812.

[28] Datta A, Johnson W. Requirements for a hydrogen powered all-electric manned helicopter. In: 12th AIAA Aviation Technology, Integration, and Operations (ATIO) Conference and 14th AIAA/ISSMO Multidisciplinary Analysis and Optimization Conference; 2012. https://doi.org/10.2514/6.2012- 5405.

[29] Saias CA, Roumeliotis I, Goulos I, Pachidis V, Bacic M. Design exploration and performance assessment of advanced recuperated hybrid-electric urban air mobility rotorcraft. J Eng Gas Turbines Power 2022;144(3):031023. https://doi.org/10.1115/1.4052955.

[30] MacMillan WL. Development of a modular type computer program for the calculation of gas turbine. PhD Thesis. Cranfield University; 1974.

[31] Padfield GD. Helicopter flight dynamics - the theory and application of flying qualities and simulation modelling. Chichester, UK: John Wiley and Sons; 2007.

[32] Leishman JG. Principles of helicopter aerodynamics. 2nd ed. New York, USA: Cambridge Aerospace Series; 2006.

[33] Bhagwat MJ. Optimum loading and induced swirl effects in hover. J Am Helicopter Soc 2015;60(1). https://doi.org/10.4050/JAHS.60.012004. URL.

[34] K. W. Mangler, Calculation of the induced velocity field of a rotor, Royal Aircraft Establishment, Report Aero 2247.

[35] Harendra PB, Joglekar MJ, Gaffey TM, Marr RL. V/STOL tilt rotor study - volume V: a mathematical model for real time flight simulation of the bell model 301 tilt rotor research aircraft, NASA contract NAS 2-6599 (Report 301-099-001).

[36] Ferguson SW. A mathematical model for real time flight simulation of a generic tilt-rotor aircraft, NASA Contractor Report (CR-166536).

[37] Maisel MD, Giulianetti DJ, Dugan DC. The history of the XV-15 tilt rotor research aircraft: from concept to flight, NASA/SP-2000-4517, NASA Ames Research Center.

[38] Carlson EB, Zhao YJ. Optimal short takeoff of tiltrotor aircraft in one engine failure, J Aircraft 39 (2). https://doi.org/10.2514/2.2925.
[39] Dreier ME. Introduction to helicopter and tiltrotor flight simulation. AIAA American Institute of Aeronautics & Astronautics; 2007. eISBN: 978-1-60086-208-3.
[40] Goulos I, Giannakakis P, Pachidis V, Pilidis P. Mission performance simulation of integrated helicopter–engine systems using an aeroelastic rotor model. J Eng Gas Turbines Power 2012;135(9):091201. https://doi.org/10.1115/1.4024869.
[41] Goulos I, Hempert F, Sethi V, Pachidis V, d'Ippolito R, d'Auria M. Rotorcraft engine cycle optimization at mission level. J Eng Gas Turbines Power 2022;135(9):091202. https://doi.org/10.1115/1.4024870.
[42] Ballin MG. A high fidelity real-time simulation of a small turboshaft engine, NASA Technical Memorandum 100991.
[43] Ames Research Center and U.S. Army air mobility R&D laboratory, NASA/Army XV-15 Tilt Rotor Research Aircraft Familiarization Document. Jan 1975.
[44] Ortiz-Carretero J, Castillo Pardo A, Goulos I, Pachidis V. Impact of adverse environmental conditions on rotorcraft operational performance and pollutant emissions, J Eng Gas Turbines Power 140 (2), 021201. https://doi.org/10.1115/1.4037751
[45] Johnson W, Branch A. NDARC — NASA design and analysis of rotorcraft. Validation and demonstration. In: American helicopter society aeromechanics specialists' conference, san fransisco, CA; 2010.
[46] Xu W, Li Q, Huang M. Design and analysis of liquid hydrogen storage tank for high-altitude long-endurance remotely-operated aircraft. Int J Hydrogen Energy 2015;40(46). https://doi.org/10.1016/j.ijhydene.2015.09.028. 16578–16586, https://www.sciencedirect.com/science/article/pii/S0360319915300367.
[47] Steels Atlas. Grade Data Sheet (304, 304L, 304H) 2011. URL, https://www.atlassteels.com.au/documents/Atlas_Grade_datasheet_304_rev_Jan_2011.pdf.
[48] Klell M. Storage of hydrogen in the pure form. John Wiley & Sons, Ltd; 2010. p. 1–37. arXiv:https://onlinelibrary.wiley.com/doi/pdf/10.1002/9783527629800.ch1.
[49] Verstraete D. The potential of liquid hydrogen for long range aircraft propulsion.. PhD Thesis. Cranfield University; 2009.
[50] Corchero G, Montañes J. An approach to the use of hydrogen in actual commercial aircraft engines. In: Proceedings of the 16th ISABE international symposium on air breathing engines, cleveland, Ohio, USA; 2003. p. 2003.1187.
[51] Simon B, Brines G, Orlov V. Joint cryogenic engine study. Int J Hydrogen Energy 1994;19(7):617–23. https://doi.org/10.1016/0360-3199(94)90221-6. URL, https://www.sciencedirect.com/science/article/pii/0360319994902216.
[52] Flange Immersion Heaters. Watlow. Specification Sheet October 2021. https://www.watlow.com/products/heaters/immersion-heaters/ansi-flange-immersion-heaters.
[53] Heaters Circulation. Watlow. Specification Sheet October 2021. https://www.watlow.com/products/heaters/circulation-heaters/38-flange-circulation-heaters-with-baffles.
[54] Poll DIA. The optimum aeroplane and beyond. Aeronaut J 2009;113(1141):151–64. https://doi.org/10.1017/S000192400001143X.
[55] Cetinkaya E, Dincer I, Naterer G. Life cycle assessment of various hydrogen production methods. Int J Hydrogen Energy 2012;37(3):2071–80. https://doi.org/10.1016/j.ijhydene.2011.10.064. 2010 AIChE Annual Meeting Topical Conference on Hydrogen Production and Storage Special Issue, https://www.sciencedirect.com/science/article/pii/S036031991102430X.
[56] Lokesh K, Sethi V, Nikolaidis T, Goodger E, Nalianda D. Life cycle greenhouse gas analysis of biojet fuels with a technical investigation into their impact on jet engine performance. Biomass Bioenergy 2015;77:26–44. https://doi.org/10.1016/j.biombioe.2015.03.005. URL, https://www.sciencedirect.com/science/article/pii/S0961953415000859.